

Rheological characterization and shape control in gel-casting of nano-sized zirconia powders

Liu, Gang; Attallah, Moataz M.; Jiang, Yun; Button, Timothy

DOI:

[10.1016/j.ceramint.2014.06.036](https://doi.org/10.1016/j.ceramint.2014.06.036)

License:

Other (please specify with Rights Statement)

Document Version

Peer reviewed version

Citation for published version (Harvard):

Liu, G, Attallah, MM, Jiang, Y & Button, T 2014, 'Rheological characterization and shape control in gel-casting of nano-sized zirconia powders', *Ceramics International*, vol. 40, no. 9 PART A, pp. 14405-14412.

<https://doi.org/10.1016/j.ceramint.2014.06.036>

[Link to publication on Research at Birmingham portal](#)

Publisher Rights Statement:

NOTICE: this is the author's version of a work that was accepted for publication in *Ceramics International*. Changes resulting from the publishing process, such as peer review, editing, corrections, structural formatting, and other quality control mechanisms may not be reflected in this document. Changes may have been made to this work since it was submitted for publication. A definitive version was subsequently published in *Ceramics International* [VOL 40, ISSUE 9, November 2014] DOI: 10.1016/j.ceramint.2014.06.036

Eligibility for repository checked October 2014

General rights

Unless a licence is specified above, all rights (including copyright and moral rights) in this document are retained by the authors and/or the copyright holders. The express permission of the copyright holder must be obtained for any use of this material other than for purposes permitted by law.

- Users may freely distribute the URL that is used to identify this publication.
- Users may download and/or print one copy of the publication from the University of Birmingham research portal for the purpose of private study or non-commercial research.
- User may use extracts from the document in line with the concept of 'fair dealing' under the Copyright, Designs and Patents Act 1988 (?)
- Users may not further distribute the material nor use it for the purposes of commercial gain.

Where a licence is displayed above, please note the terms and conditions of the licence govern your use of this document.

When citing, please reference the published version.

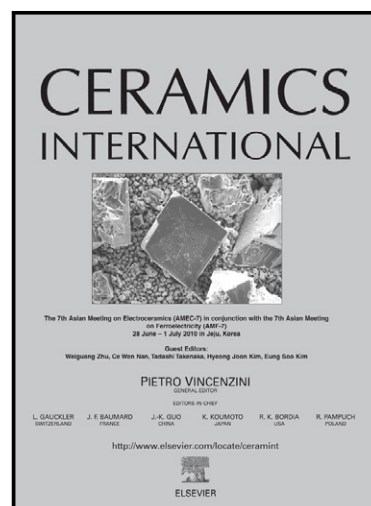
Take down policy

While the University of Birmingham exercises care and attention in making items available there are rare occasions when an item has been uploaded in error or has been deemed to be commercially or otherwise sensitive.

If you believe that this is the case for this document, please contact UBIRA@lists.bham.ac.uk providing details and we will remove access to the work immediately and investigate.

Rheological characterization and shape control in gel-casting of nano-sized zirconia powders

Gang Liu, Moataz M Attallah, Yun Jiang, Tim W Button



www.elsevier.com/locate/ceramint

PII: S0272-8842(14)00930-4
DOI: <http://dx.doi.org/10.1016/j.ceramint.2014.06.036>
Reference: CERI8721

To appear in: *Ceramics International*

Received date: 23 March 2014
Revised date: 5 June 2014
Accepted date: 6 June 2014

Cite this article as: Gang Liu, Moataz M Attallah, Yun Jiang, Tim W Button, Rheological characterization and shape control in gel-casting of nano-sized zirconia powders, *Ceramics International*, <http://dx.doi.org/10.1016/j.ceramint.2014.06.036>

This is a PDF file of an unedited manuscript that has been accepted for publication. As a service to our customers we are providing this early version of the manuscript. The manuscript will undergo copyediting, typesetting, and review of the resulting galley proof before it is published in its final citable form. Please note that during the production process errors may be discovered which could affect the content, and all legal disclaimers that apply to the journal pertain.

Rheological Characterization and Shape Control in Gel-Casting of Nano-sized Zirconia Powders

Gang Liu^{a,b}, Moataz M Attallah^b, Yun Jiang^{b*} and Tim W Button^b

a. Faculty of Materials and Energy, Southwest University, 400715, Chongqing, P.R.China

b. School of Metallurgy and Materials, The University of Birmingham, Edgbaston, B15 2TT U.K.

Abstract

In this study, a water soluble resin based gel system was developed incorporating nano-sized zirconia powders. The effects of the resin content and the solid loading on the rheological properties, density, mechanical properties and shape control have been investigated. All the slurries show typical shear-thinning behaviour. Higher resin-content leads to higher viscosity and larger green density. The density of the green component obtained from a slurry with 30 wt.% resin can reach 2.85 g/cm³ (nearly 50% of the theoretical density). However, when the resin content is beyond 25 wt.%, the sintered density decreased. Higher density, solid-loading and applying external force are helpful to improve the shape control.

Key words: Rheological property; Gel-casting; Nano-sized zirconia; Shape control

1. Introduction

Nano-sized powders have attracted much attention in the past decades due to the significant improvement in key properties. Zirconia nano-particles have thus become one of the most important ceramic materials, for example, they can provide an effective way to lower thermal conductivity in thermal barrier coatings[1]. Moreover, ZrO₂ is a prevalent biomaterial in dentistry and dental implantology.

However, microstructural control is essential if specific requirements need to be fulfilled. The fabrication process plays an important role in the control of the microstructure as well as the shape

*Yun Jiang, Corresponding author. School of Metallurgy and Materials, The University of Birmingham, Edgbaston, U.K. B15 2TT. Email: y.jiang.1@bham.ac.uk

Gang Liu, Faculty of Materials and Energy, Southwest University, Chongqing, China, 400715. Tel: 0086 23 68254376. Fax: 0086 23 68254376. Email: liugangxjtu@gmail.com.

[2,3]. Gel casting[4], a commercial colloidal process[5], is relatively new and very attractive for manufacturing high-quality ceramics with homogeneous microstructures and complex shapes. It is actually a moulding technique using an in-situ polymerisation process to immobilise the ceramic powders and to allow them to hold the shape of the mould[6]. Different gel casting systems have been studied since it was first developed in Oak Ridge National Laboratory in the 1990s[7,8]. However, each system has its own drawbacks, for example, the free radical polymerisation of monomer and cross linker will be inhibited by the oxygen in the frequently used system, leading to surface-exfoliation of the green compact[9]. Although the processing systems based on coordinative or biopolymer chemistry could be carried out in air, the resulting slurries and samples show high viscosity and poor green strength, respectively[5], limiting their further application. In recent years, a ring-open polymerisation mechanism based on the poly-addition reaction between a water-soluble epoxy resin and amine hardener has been introduced in the gel casting technique, allowing the gel to be processed in air[10,11]. However, this technique is still in its early stage and few studies are incorporated nano-sized powders. Therefore, the purpose of the present investigation is to develop a water-soluble epoxy resin based gel system suitable for nano-sized ZrO_2 powders.

2. Experimental

2.1 Raw Materials

A commercial yttria-stabilized zirconia powder (Tosoh-zirconia, Japan) was used as the ceramic powder. Ethylene glycol diglycidyl ether (EGDE, Sigma-Aldrich, Germany) and bis (3-aminopropyl) amine (Sigma-Aldrich, Germany) were used as epoxy resin (monomer) and hardener, respectively. Specially, the weight ratio of the resin content and the hardener content was fixed at 1:0.23 for all slurries. 0.86 ml ammonium polyacrylate (NH_4PAA) solution (Allied Colloids, Bradford, UK) per 100 g powder was added as the dispersant. Distilled water ($17 \text{ M}\Omega\cdot\text{cm}$) was used as the vehicle.

2.2 Processing

An aqueous solution containing EGDE was prepared by dissolving the epoxy resin into the mixture of distilled water and dispersant prior to the preparation of slurries. Afterwards, slurries with various solids loading (30, 35, 40, 45vol.%) were prepared by adding zirconia powders into the premixed solution under constant stirring. Slurries were ball milled for 24 hours with zirconia milling media. Hardener was added into the slurries and mixed. The resulting slurries were then poured into suitable silicone moulds with desired shapes and degassed in a vacuum system for 1 minute to aid moulding and de-airing. After drying at room temperatures for 24 hours, demoulding was carefully done and the green bodies were transferred into a 40 °C oven for further drying for next 24 hours. Sintering was carried out in air. A slow ramp of 1 °C/min to 600 °C was conducted to burn out the polymer followed by 5 °C/min ramp to 1550 °C, where it was held for 2 hours. Samples were ground and polished for observation and measurement.

2.3 Characterization

The rheological behaviour was characterised with an AR 500 rheometer (TA instruments, USA) with a cone and plane system (Truncation: 59 µm; Core: 4 cm, 2°). A solvent trap was coupled to the measuring unit to prevent evaporation. The gelation behaviour of the zirconia slurries with varying resin contents was studied by monitoring the evolution of the viscosity under a constant shear of 0.1 s⁻¹ at 20 °C. The criterion used for the gel time measurement is based on the classical theory that one of the attributes of the gel point is an infinite steady-shear viscosity [12]. The flow behaviour of the slurries was measured at 20 °C under the continuous shear mode within the shear rate range of 600 s⁻¹ (from 0.1 up to 600 s⁻¹) in 90 seconds. All the rheological characterization started immediately after the addition of hardener. All the densities in this study were measured by Archimedes method. The Vickers microhardness test was performed on the sintered sample using a Mitutoyo MVK-H1 microhardness tester (1 kg load for ten seconds) (Mitutoyo Ltd, UK). An optical digital camera (Olympus SP350, Olympus Co (UK) Ltd) was used to record the shape of the

green components. Scanning Electron Microscopy (SEM) (JSM 7000, Jeol, Tokyo, Japan) was employed to observe the microstructure of green and sintered samples.

3. Results and discussion

3.1 Influence of Experimental Variables on Properties

A secondary electron SEM micrograph of the zirconia powder used in this investigation is shown in Fig.1 and it can be seen that the powder has a near-spherical morphology with a primary particle size around 100 nm.

Fig. 2(a) shows the effect of the various resin contents on the rheological properties of the slurries with 35vol.% solids loading. All the slurries showed shear thinning behaviour within the measurement range. As the resin content increased from 15 wt.% to 30 wt.%, the viscosities of zirconia suspensions increased at the same shear rate, especially when the shear rate is low (below 40 1/s). The viscosity of the resin used in this study at 20 is 20 mPa·s (from the product information), which is much larger than that of water (1.002 mPa·s). So, the viscosity of the slurry system including water, powder, dispersant and resin, will arise with the increase of the resin content. Meanwhile, according to our observation during the hardener mixing and slurry casting process, the hardener is very helpful to lower the viscosity of this slurry system (the fluidity became better after adding hardener). As mentioned in the experimental section, the ratio of resin (monomer) to hardener (coupling reagent) was 1:0.23 (wt.%). More resin added means more hardener needed. It is probably that the effect of resin content on viscosity dominated when the resin content increased from 15wt.% to 20wt.%, so the viscosity of the slurry system increased. However, the effect of hardener addition on viscosity had a peak value under this fixed solids loading of 35 vol.%. Therefore, when the resin content increased from 20wt.% to 25wt.%, the effect of hardener on viscosity gradually played an important role (actually under the two action mechanisms just mentioned), so the viscosity of 20wt.% curve is close to that of 25wt.% curve. With further addition

of resin content to 30wt.%, the effect of resin content on viscosity started to dominate again. Hence, the slurry with 30wt.% resin content showed the highest viscosity.

The idle time is defined as the time after which the gelation begins. It is an important parameter in the gelcasting process. If the idle time is too short, i.e. ≤ 10 minutes, the gelation will occur when mixing hardener in the ceramic slurry; if it is too long, i.e. ≥ 70 minutes, it is not feasible from the economical point of view[13]. Therefore, the idle time should be optimized. Fig.2(b) shows the viscosity as a function of time for the 35vol.% slurries with various resin contents. It is found that all the curves possess a period with constant viscosity, then the viscosities in all curves start to increase gradually until they begin to increase rapidly towards infinity. The period with constant viscosity is defined as the idle time in the polymerization process, which is the available time that can be used for casting[14]. As shown in Fig.2(a), the idle time of the slurries decreased from about 1350 s to 900 s when the resin content increased from 15 wt.% to 30wt.%. The decrease of the idle time was mainly attributed to the “container” effect of the slurry in the presence of ceramic powders according to Dong’s work[15]. For the slurry gelation, polymer chain lines are needed to connect the ceramic particles and fill the interstices of the particles in the slurry, for which a certain period of time is required (the idle time). The idle time depends on the size of the “container”: the smaller the “container”, the shorter time the polymer chain line is needed to connect the particles. When the resin content is increased, the space between the particles in the slurry (the vehicle (water) content is fixed) is reduced leading to a reduction of the “container” size, which finally results in the decrease of the idle time. Therefore, higher resin content leads to shorter idle time, which is in agreement with Olhero’s investigation [16]. Moreover, one interesting phenomenon is that figure 2(b) shows a neat difference in the idle time between these systems with different resin contents (15-20 wt.% vs 25-30 wt.%). Probably, for this epoxy-hardener system, when the resin content is over 20 wt.%, the ‘container’ size will dramatically decrease, finally resulting in the neat difference.

Fig. 2(c) shows the effects of solid loadings on the rheological properties of the slurries with 15wt.% resin content. All the slurries tested here showed typical shear thinning behaviour within the measurement range. Viscosities increased dramatically with increase of solid loadings from 30 vol.% to 45 vol.%. Figure 3 show the dispersion status of zirconia powders in these slurries. Due to the relatively low solids loading (30 vol.%), the powders in Figure 3(a) exhibits a good dispersion status. However, evident aggregates can be observed, especially when the solids loading increased to 45 vol.%, as shown in Figure 3(b) and Figure 3(c) (red circles). That is because significant increase of the attractive potential energy due to long-range van der Waals interactions between particles when the solids loading arises especially using this nano-sized zirconia powders. Therefore, the presence of attractive interparticle interactions and the formation of particle aggregates resorts into higher values and stronger concentration dependence of viscosity. Similar results can be found in Tan's and Chen's work [17,18].

Table 1 summaries the physical properties of the green and sintered components consolidated by this aqueous gel casting technique. For the 35 vol.% slurry, with increase of the resin content from 15 wt.% to 30 wt.%, the density of the green component increased. This behaviour occurs because a 3D network of fine pores will be generated during gelation, which can exert high suction pressure on drying resulting in the shrinkage of gelcast samples[16]; higher resin content leads to enhanced fineness of the 3D network pores, which gives stronger capillary forces making the particles approach each other more upon drying. The increased fraction of the resin filling the interstitial pores particles also contributes to the increase of the green density with increase of the resin content. These two effects result in the increase of the green density.

Fig. 4(a)-(d) show the secondary electron SEM micrographs of the green samples with different amounts of epoxy resin. Due to the small change of the densities as shown in Table 1, the variation of the porosity is not obvious in these SEM images. The sintered densities showed a different trend compared with the green densities. When the added amount of the resin was more than 25 wt.%, the

sintered density started to decrease, indicating that high resin content over 25 wt.% is detrimental to the sintering behaviour. When the resin content increased from 15 wt.% to 30 wt.%, the microhardness showed a very similar trend to the sintered density, as shown in Table 1.

The effect of solid-loading has also been investigated as shown in Table 1. With increase of the solid-loading from 35 vol.% to 45 vol.% with 15 wt.% resin content, the density of the green component increased from 2.69 g/cm³ to 3.02 g/cm³. Moreover, the sintered density and the microhardness reported in Table 1 for these samples showed the same trend when the solid loading increased. The sintered density increased from 5.28 g/cm³ (89% relative density) to 5.45 g/cm³ (92% relative density) and the microhardness increased from 13.3 GPa to 14.2 GPa, similar to that reported in Tulliani's work[19] (14.3GPa, 95% relative density). A gradual decrease of the density of pores was found, as can be seen in Fig. 5 (a), (b) and (c), which show the microstructure of the fracture surface of these samples. Accordingly, with increase of the solid loading, a denser microstructure could be observed. Therefore, higher solid loading is helpful to improve the density which would be expected to improve the mechanical properties, which is consistent with Chen's investigation[18].

3.2 Influence of Experimental Variables on Shape Control

Two microgears in the green state fabricated from slurries with 35 vol.% solid-loading and 15 wt.% resin content are shown in Fig. 6. It can be seen that the right microgear shows more defects than the left one, although the left one does have several defects. The only difference between the two is the PDMS mould used for manufacturing the gear shown in figure 6(a) was bent slightly after casting. Bending the PDMS mould slightly allows the slurry to fill the mould fully and reproduce the very fine structure of the mould accurately.

Several long bars in the green state produced from slurries with 35 vol.% solid-loading and different resin contents are shown in Fig. 7. Bending the PDMS moulds by hand was applied here. It can be observed that with increase of the resin content from 15 wt.% (right hand side) to 25 wt.%

(middle one), the surface of the samples becomes much smoother and the edges become much sharper. This is mainly because the sample with 15 wt.% resin content has the lower density (as shown in Table 1), resulting in lower mechanical strength of the green component. However, the long bars obtained from slurries with 25 wt.% and 30 wt.% (left hand side) resin content do not show much difference. This is because the two green components show very similar densities. Thus, higher resin content (no more than 30 wt.%) is needed for preparing green component with few drawbacks.

Based on the above results, bending the mould and adopting less than 30 wt.% resin content are applied in the following work. One microgear and spanner in the green state fabricated from slurry with 40 vol.% solid-loading and 15 wt.% resin content are shown in Fig. 8. It can be seen clearly that the surface of these samples becomes much smoother and the edges become much sharper compared to that of the sample shown in Fig.6. According to Table 1, the density of the sample obtained from 40 vol.% slurry is bigger than that of sample obtained from 35 vol.% slurry. Thus, high solid-loading is very helpful to improve the shape control, leading to much better green components.

4. Conclusions

In summary, a water-soluble epoxy resin based gel system was developed incorporating nano-sized zirconia powders and different shapes were produced by using such system. With increase of the resin content from 15 wt.% to 30 wt.%, the viscosity of the slurry increased and the idle time became shorter from about 1350 s to 900 s. Higher resin content is helpful to improve the green density and also the shape control, but not suitable for casting process. Moreover, the sintered density decreased when the resin content was beyond 25 wt.%. High solid-loading leads to high green and sintered density, which is also better for the shape control. In addition an external force, such as bending by hand, is necessary for shape control in order to reproduce the fine structure of the mould.

References

- [1] K. Jiang, S.B. Liu, C.C. Li, Nano-nano composite powders of lanthanum zirconate and yttria-stabilized zirconia by spray pyrolysis, *J Am Ceram Soc* 96(10) (2013) 3296-3303.
- [2] C. Gomez-Yanez, H. Balmori-Ramirez, F. Martinez, Colloidal processing of BaTiO₃ using ammonium polyacrylate as dispersant, *Ceram Int* 26(6)(2000) 609-616.
- [3] G. Liu, D. Zhang, T.W. Button, Preparation of concentrated barium titanate suspensions incorporating nano-sized powders, *J Eur Ceram Soc* 30 (2) (2010) 171-176.
- [4] W.M. Sigmund, N.S. Bell, L.Bergstrom, Novel powder-processing methods for advanced ceramics, *J Am Ceram Soc* 83(7) (2000) 1557-1574.
- [5] J.A. Lewis, Colloidal processing of ceramics, *J Am Ceram Soc* 83 (10) (2000) 2341-2359.
- [6] R. Gilissen, J.P. Erauw, A. Smolders, E. Vanswijgenhoven, J. Luyten, Gelcasting, a near net shape technique, *Materials & Design* 21(4) (2000) 251-257.
- [7] O.O. Omatete, M.A. Janney, R.A. Strehlow, Gelcasting - A new ceramic forming process, *American Ceramic Society Bulletin* 70 (10) (1991)1641-&.
- [8] A.C. Yong, O.O. Omatete, M.A. Janney, P.A. Menchhofer, Gelcasting of Alumina, *J Am Ceram Soc* 74 (3) (1991) 612-618.
- [9] J.S. Ha, Effect of atmosphere type on gelcasting behavior of Al₂O₃ and evaluation of green strength, *Ceram Int* 26 (3) (2000) 251-254.
- [10] X.J. Mao, S.Z. Shimai, M.J. Dong, S.W. Wang, Gelcasting of alumina using epoxy resin as a gelling agent, *J Am Ceram Soc* 90 (3) (2007) 986-988.
- [11] X.J. Mao, S.Z. Shimai, M.J. Dong, S.W. Wang, Investigation of new epoxy resin for the gelcasting ceramics, *J Am Ceram Soc* 91 (4) (2008) 1354-1356.
- [12] M.A. Rao, *Rheology of fluid and semisolid foods*. Springer, 2007.

- [13] M. Szafran, P. Wieceńska, A. Szudarska, T. Mizerski, New multifunctional compounds in gelcasting process-introduction to their synthesis and application, *J Aus Ceram Soc* 49 (1) (2013) 1-6.
- [14] X.G. Xu, Z.Y. Wen, X.W. Wu, J. Lin, X.Y. Wang, Rheology and chemorheology of aqueous γ -LiAlO₂ slurries for gel-casting, *Ceram Int* 35 (2009) 2191-2195.
- [15] M.J. Dong, X.J. Mao, Z.Q. Zhang, Q. Liu, Gelcasting of SiC using epoxy resin as gel former, *Ceram Int*, 35 (4) (2009) 1363-1366.
- [16] S.M. Olhero, L. Garcia-Gancedo, T.W. Button, F.J. Alves, J.M.F. Ferreira, Innovative fabrication of PZT pillar arrays by a colloidal approach. *J Eur Ceram Soc* 32 (5) (2012) 1067-1075.
- [17] Q.Q. Tan, Z.T. Zhang, Z.L. Tang, S.H. Luo, K.M. Fang, Influence of polyelectrolyte dispersant on slip preparation of nano-sized tetragonal polycrystals zirconia for aqueous-gel-tape-casting process, *Mater Chem Phys* 80 (3) (2003) 615-619.
- [18] B.Q. Chen, D.L. Jiang, J.X. Zhang, M.J. Dong, Q.L. Lin, Gel-casting of beta-TCP using epoxy resin as gelling agent, *J Eur Ceram Soc* 28 (15) (2008) 2889-2894.
- [19] J.M. Tullinai, C. Bartuli, Bemporad, V. Naglieri, M. Sebastiani, Preparation and mechanical characterization of dense and porous zirconia produced by gel casting with gelatin as a gelling agent, *Ceram Int* 35(6)(2009) 2481-2491.

Table 1 Physical property of the green and sintered samples

Solid-Loading [vol.%]	Resin Content [%]	Green Density[g/cm ³]	Sintered Density [g/cm ³]	Microhardness[GPa] after sintering
35	15	2.69	5.28	13.34±0.50
35	20	2.66	5.16	12.45±0.57
35	25	2.84	5.40	14.08±0.38

35	30	2.85	5.36	13.76±0.62
40	15	2.75	5.30	13.84±0.21
45	15	3.02	5.45	14.18±0.43

Captions

Figure 1. Secondary electron SEM image of the zirconia powders used in this study.

Figure 2. Rheological properties of the slurries: (a) Typical rheological flow behaviour of the 35 vol.% zirconia slurries with various resin contents; (b) Viscosity of 35vol.% zirconia slurries with different resin contents as a function of time; (c) Rheological flow behaviour of the zirconia slurries with various solids loading.

Figure 3. The dispersion status of zirconia powders in these slurries with different solids loadings (a) 35 vol.% with 15 wt.% resin; (b) 40 vol.% with 15 wt.% resin ;(c) 45 vol.% with 15 wt.% resin.

Figure 4. Secondary electron SEM micrographs of the fracture surface of the green gelcast bodies obtained from different slurries (a) 35 vol.% with 15 wt.% resin; (b) 35 vol.% with 20 wt.% resin; (c) 35 vol.% with 25 wt.% resin; (d) 35 vol.% with 30 wt.% resin; (e) 40 vol.% with 15 wt.% resin ;(f) 45 vol.% with 15 wt.% resin.

Figure 5. (a) to (c) Secondary electron SEM images of sintered samples obtained from slurries with different solid-loading but with the same resin content of 15 wt.% (a)35 vol.%; (b) 40 vol.%; (c) 45vol.%.

Figure 6. Green components obtained from slurry of 35 vol.% solid-loading and 15 wt.% resin: (left) with bending, (right) without bending.

Figure 7. Green components obtained from 35 vol.% solid-loading slurries with different resin contents 30 wt.% (left hand side), 25 wt.% (middle), 15 wt.% resin (right hand side).

Figure 8. Green components obtained from slurries with 40 vol.% solid-loading and 15 wt.% resin content

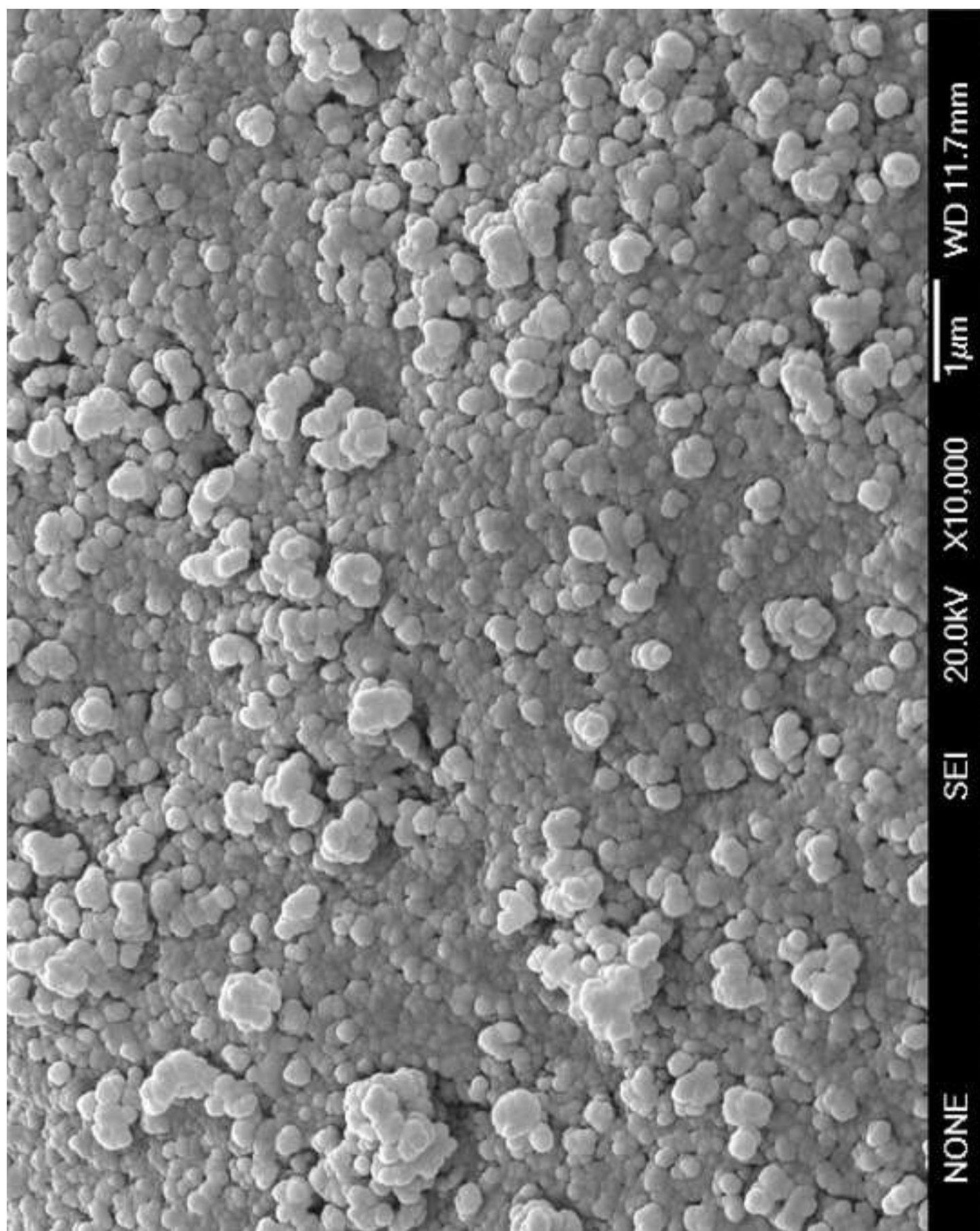


Figure 1

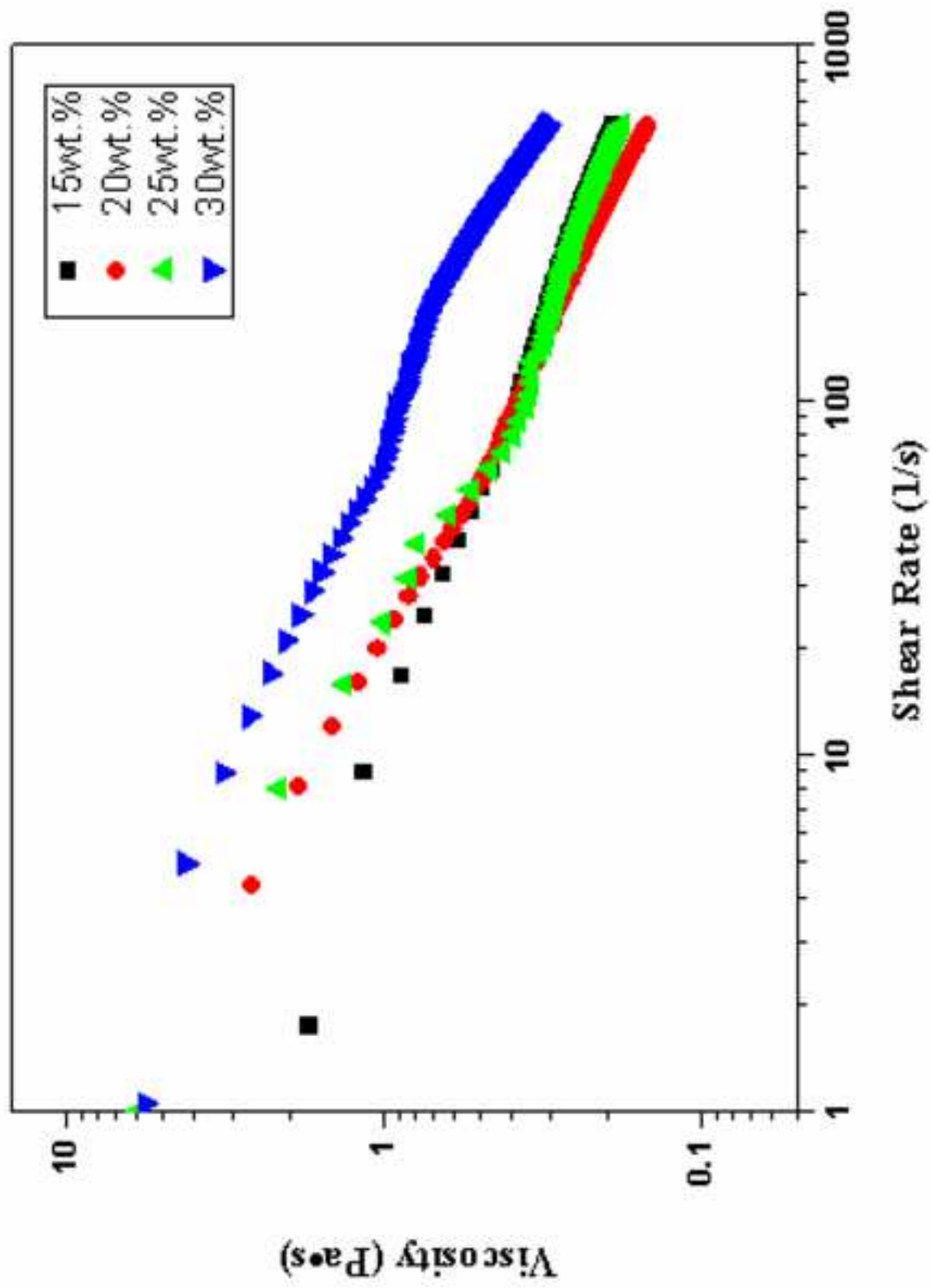


Figure 2(a)

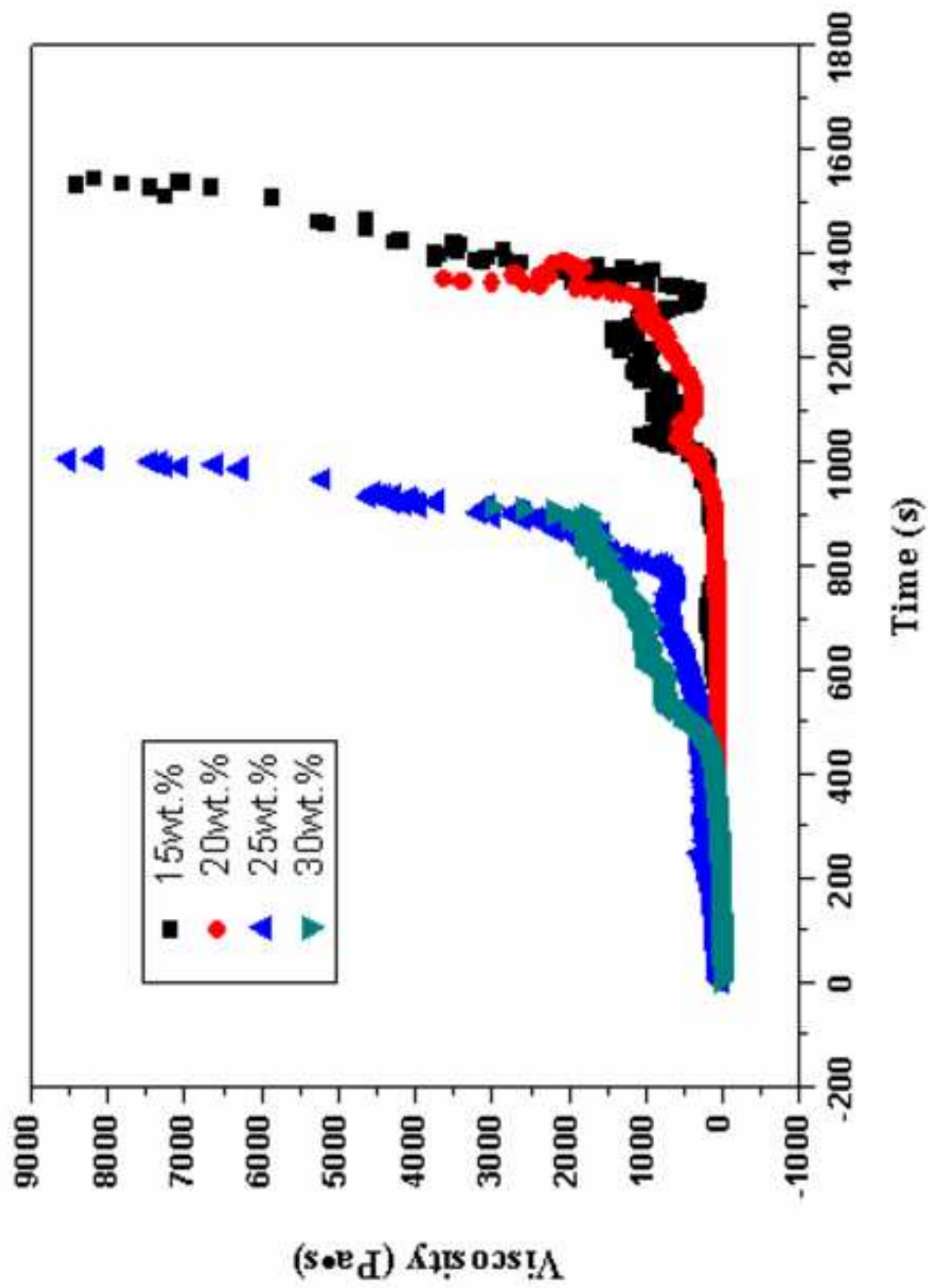


Figure 2(b)

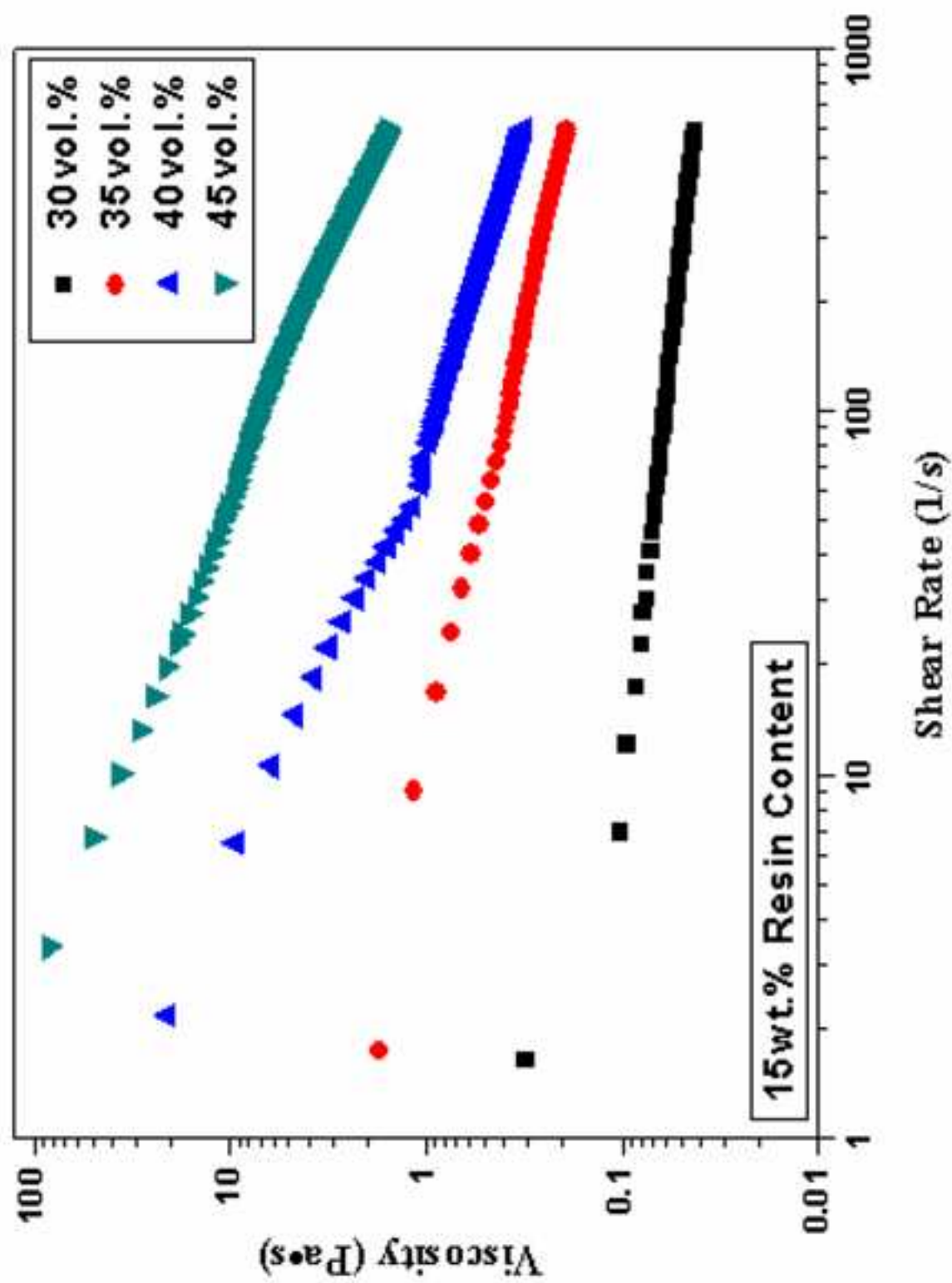


Figure 2(c)

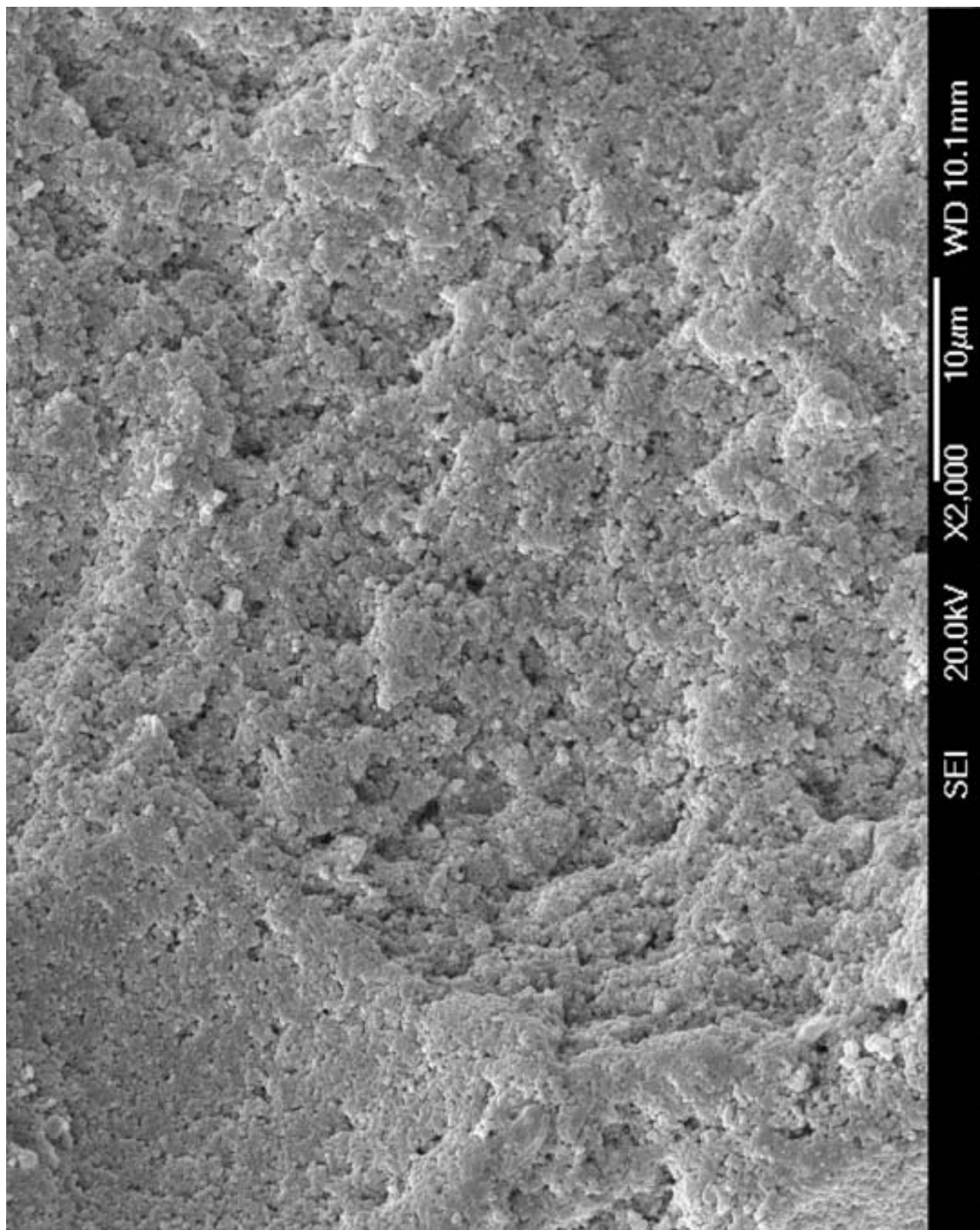


Figure 3(a)

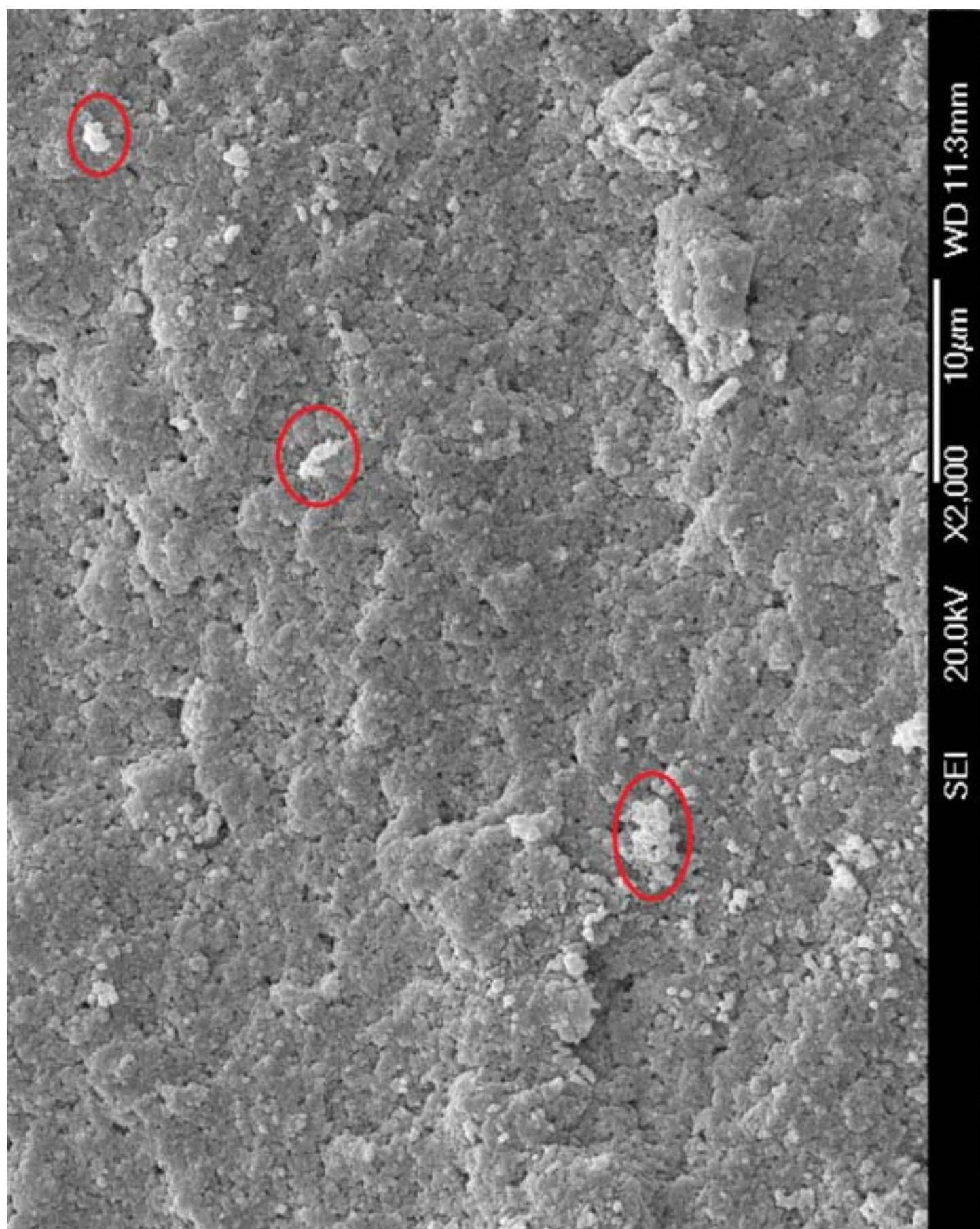


Figure 3(b)

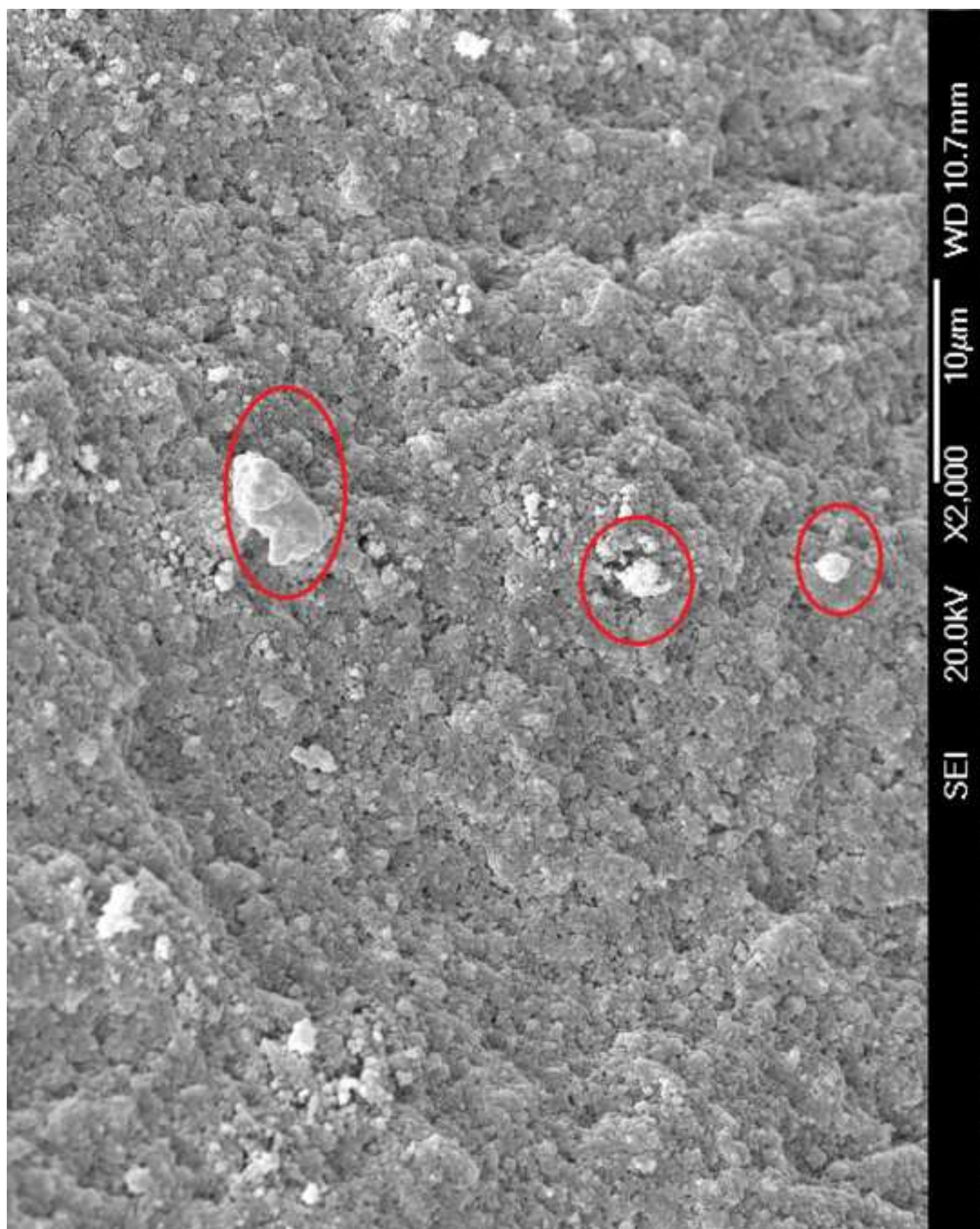


Figure 3(c)

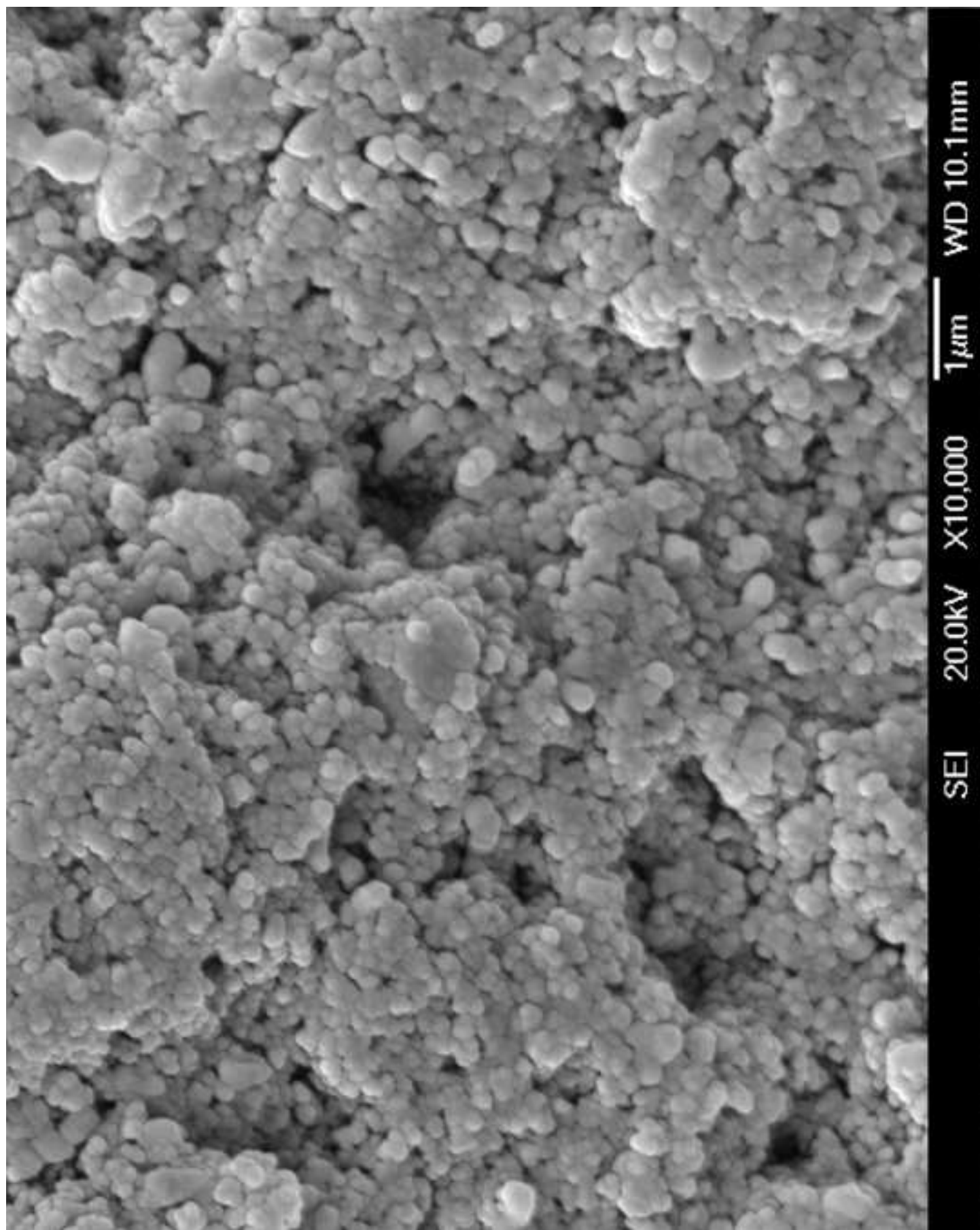


Figure 4(a)

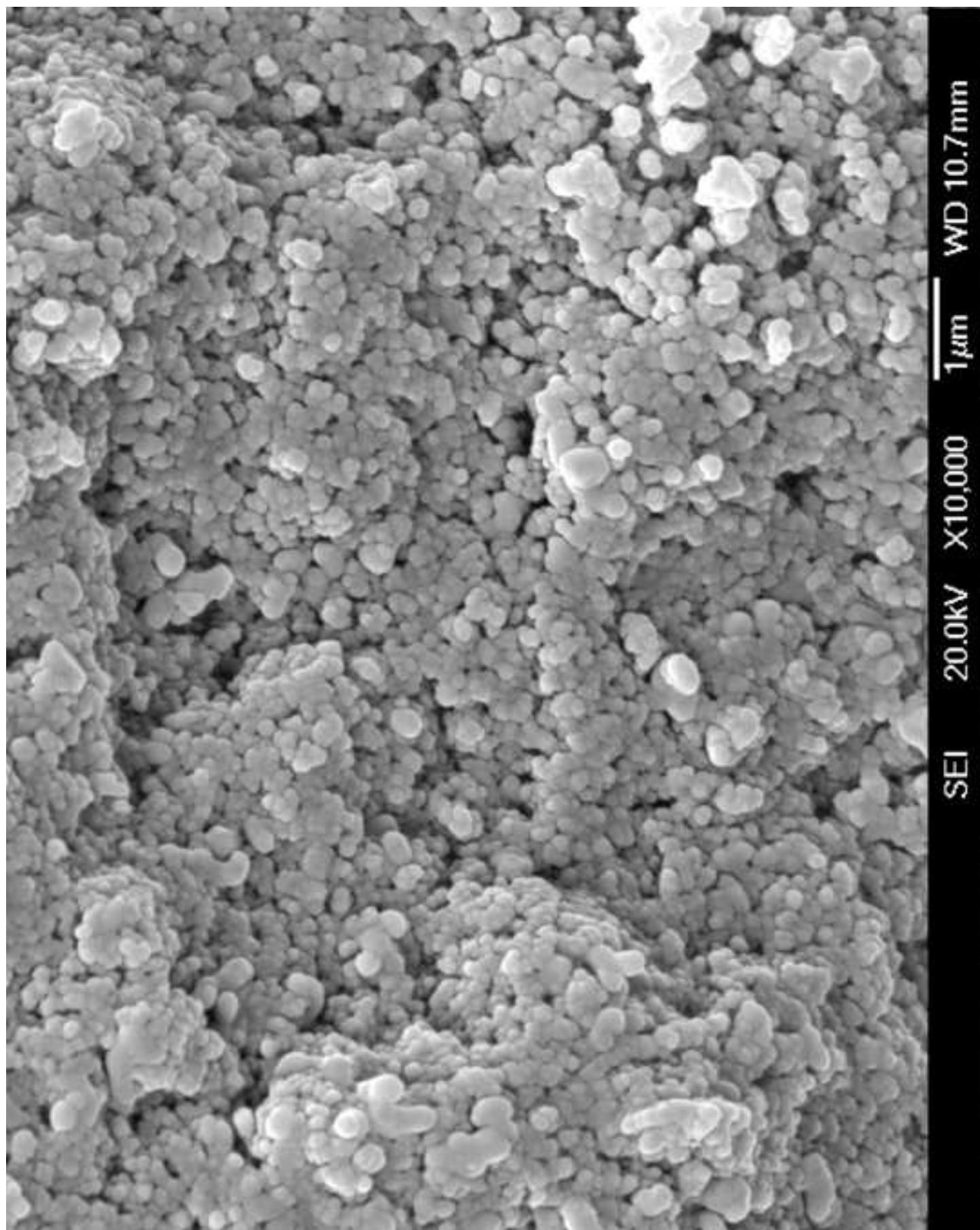


Figure 4(b)

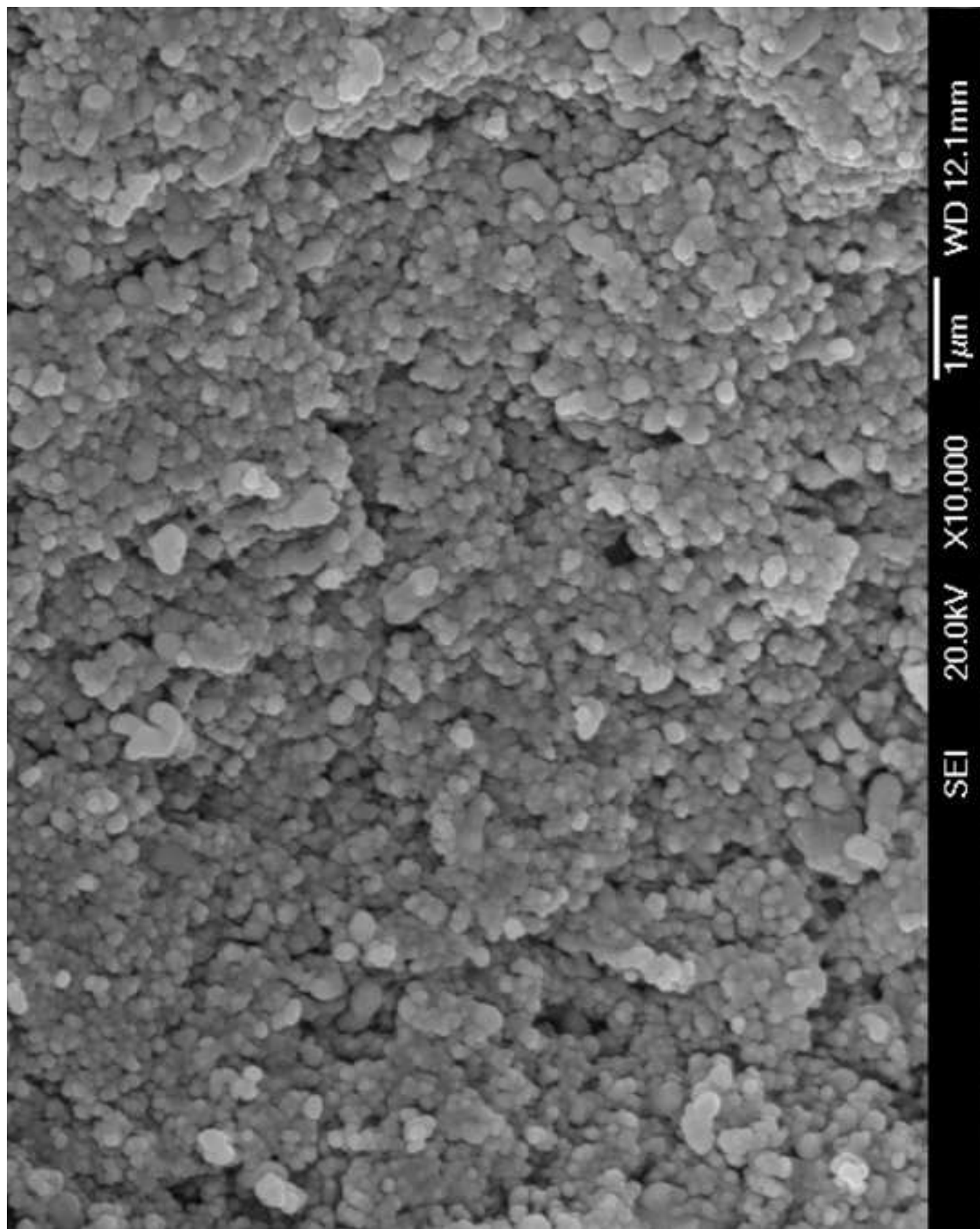


Figure 4(c)

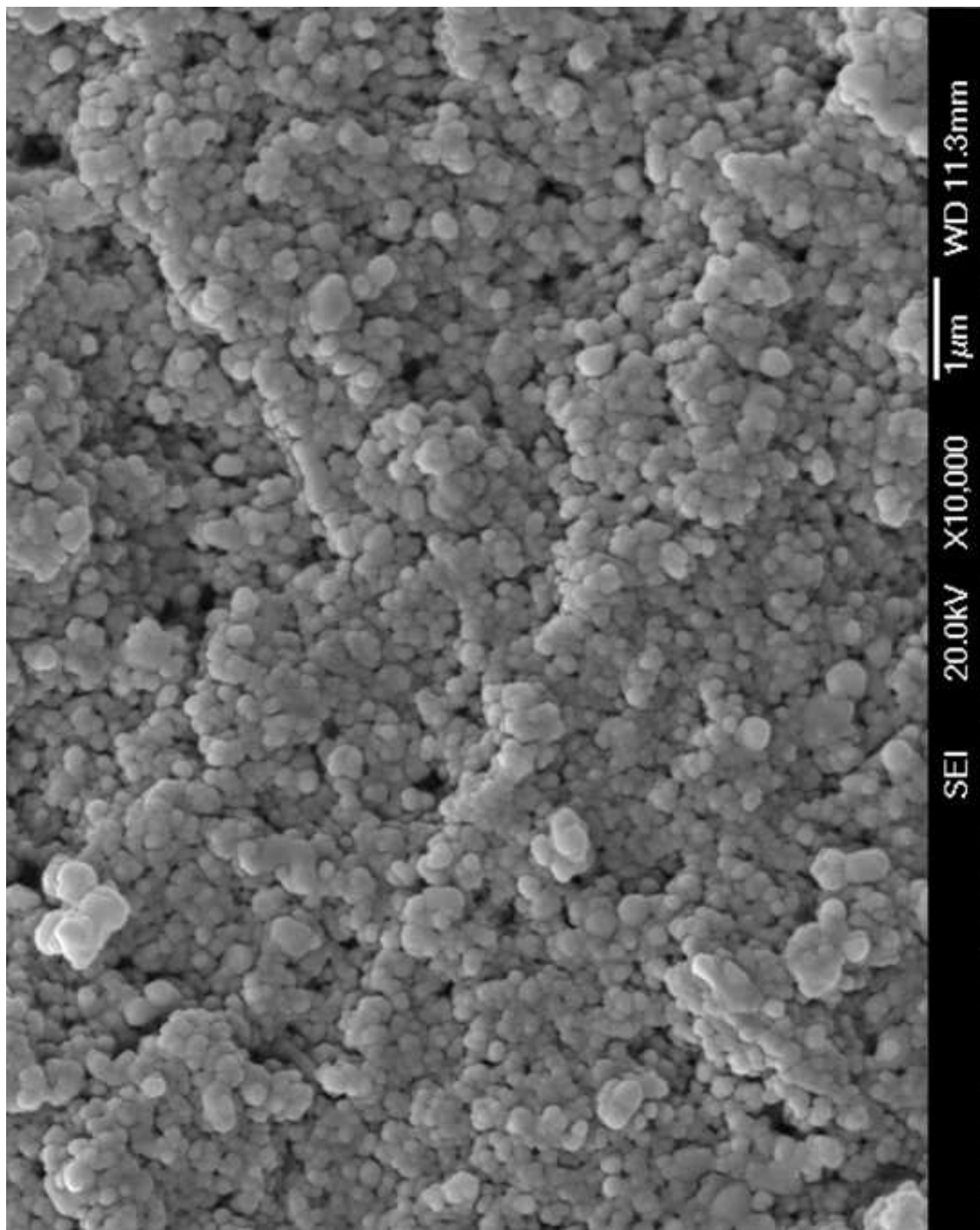


Figure 4(d)

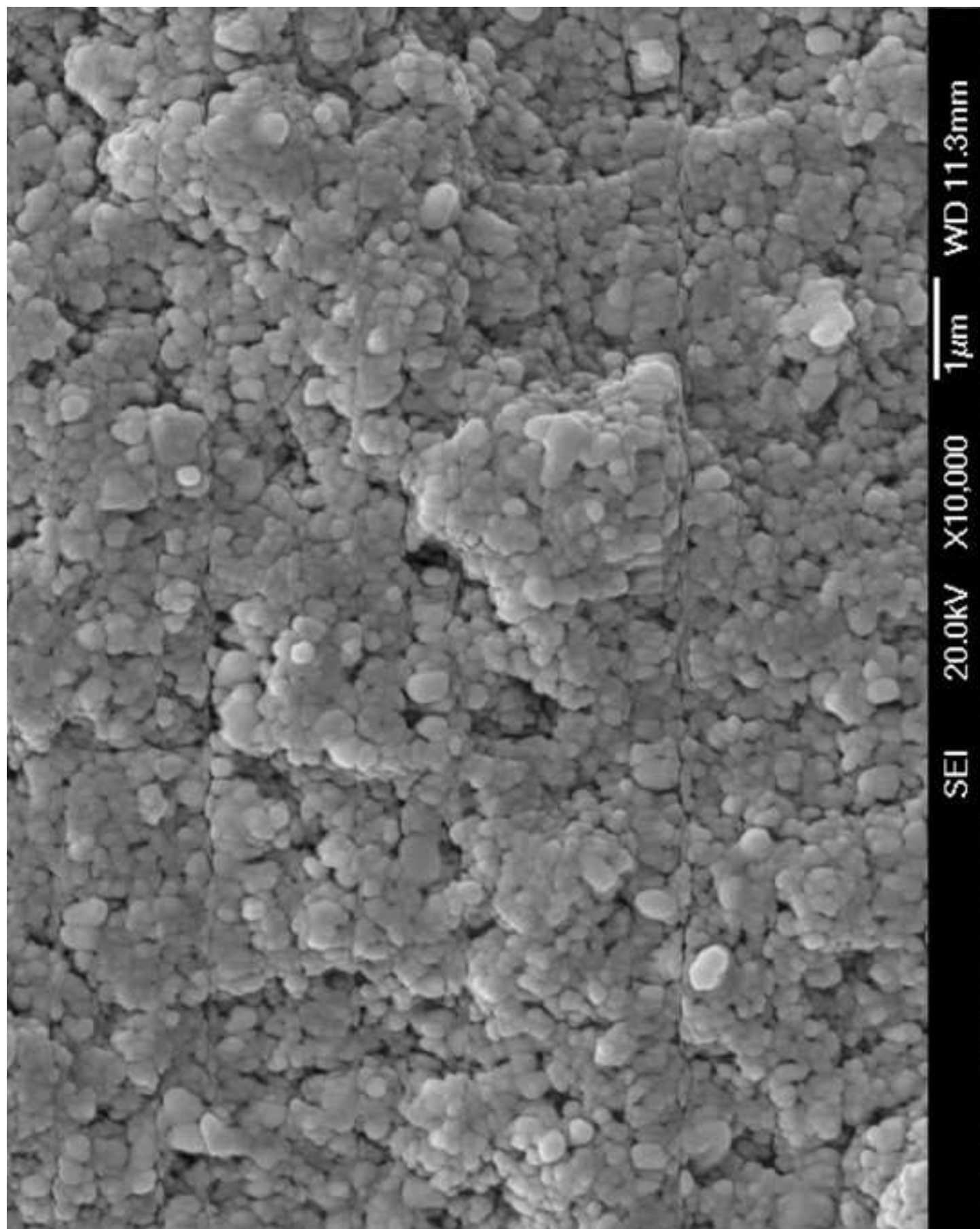


Figure 4(e)

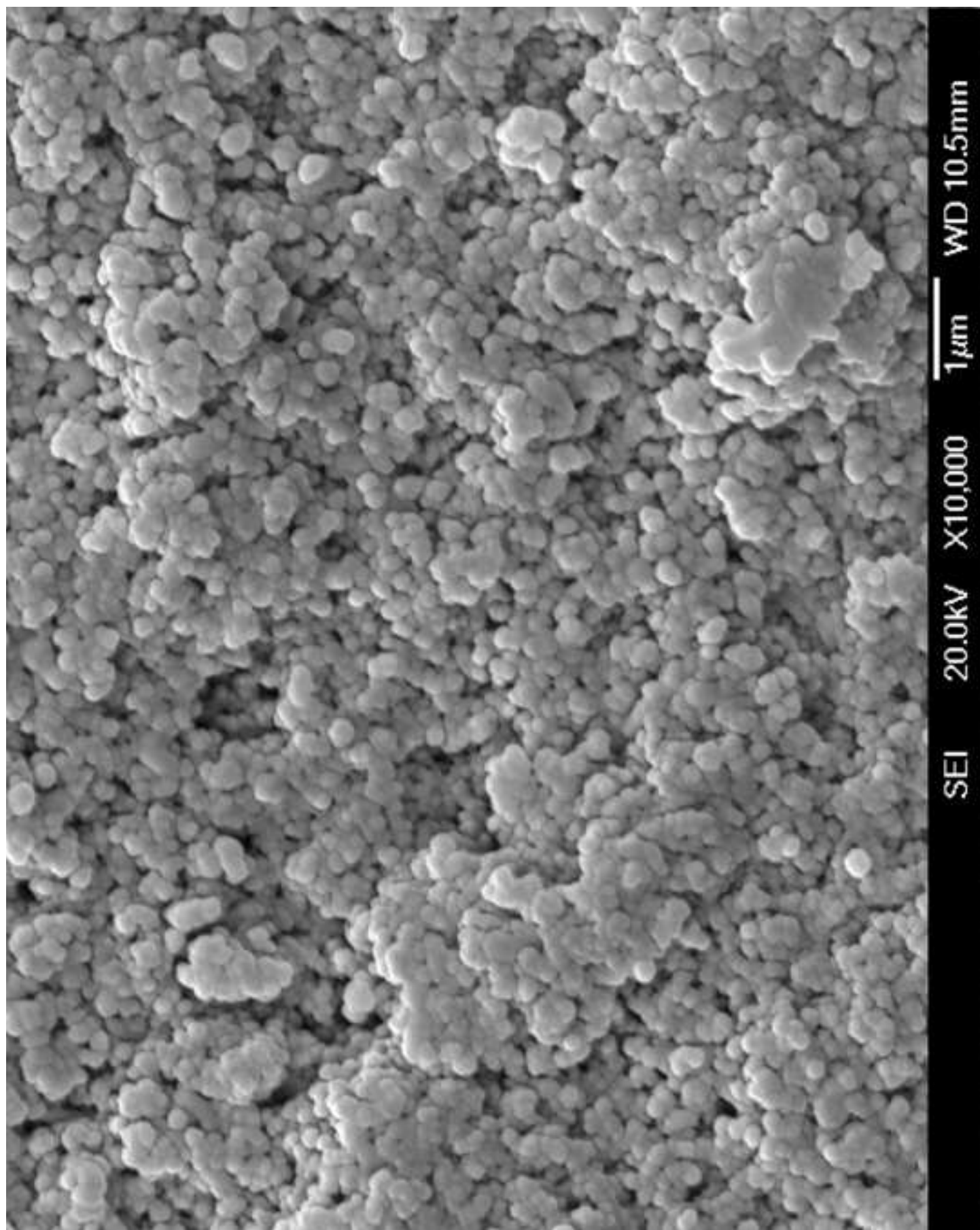


Figure 4(f)

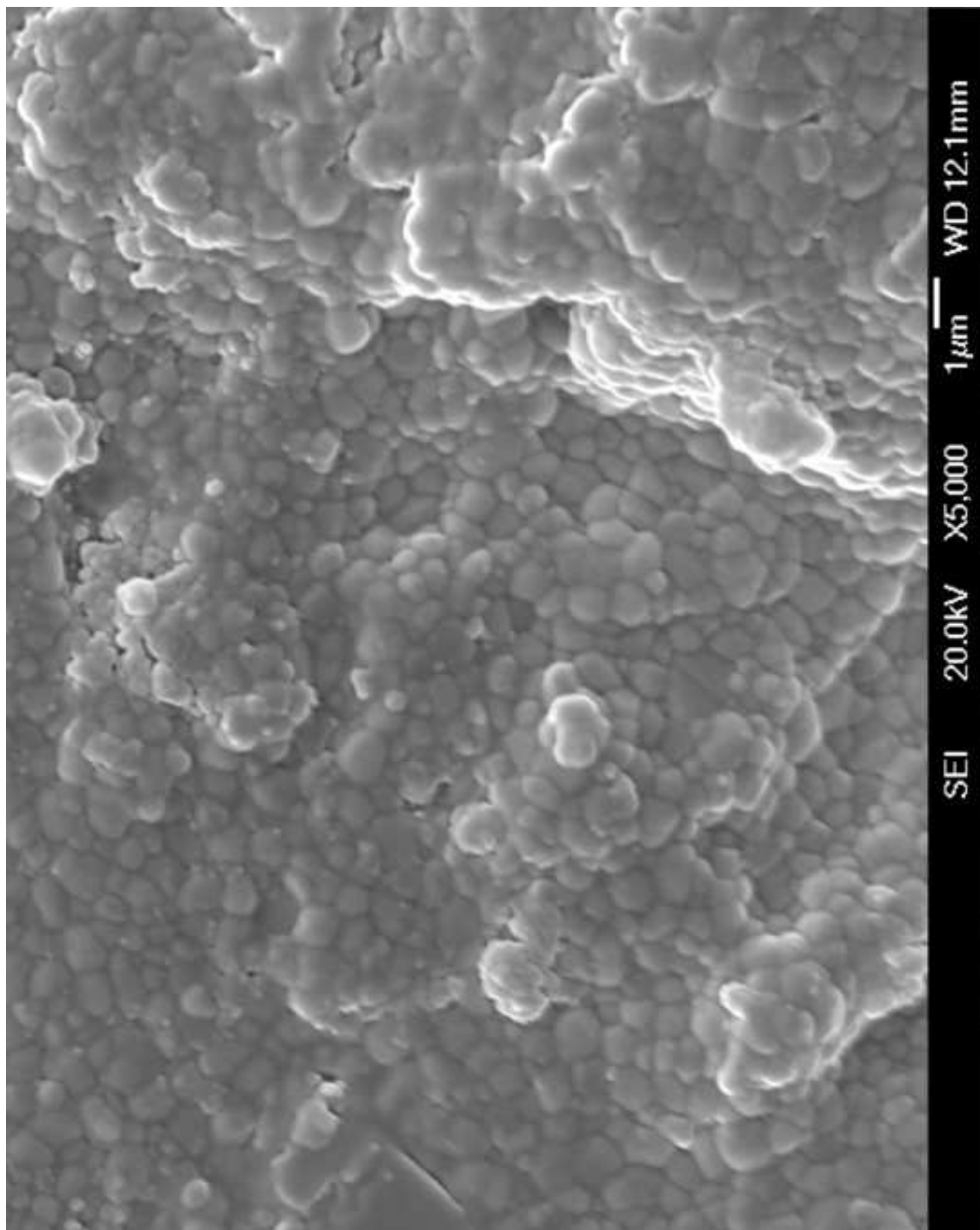


Figure 5(a)

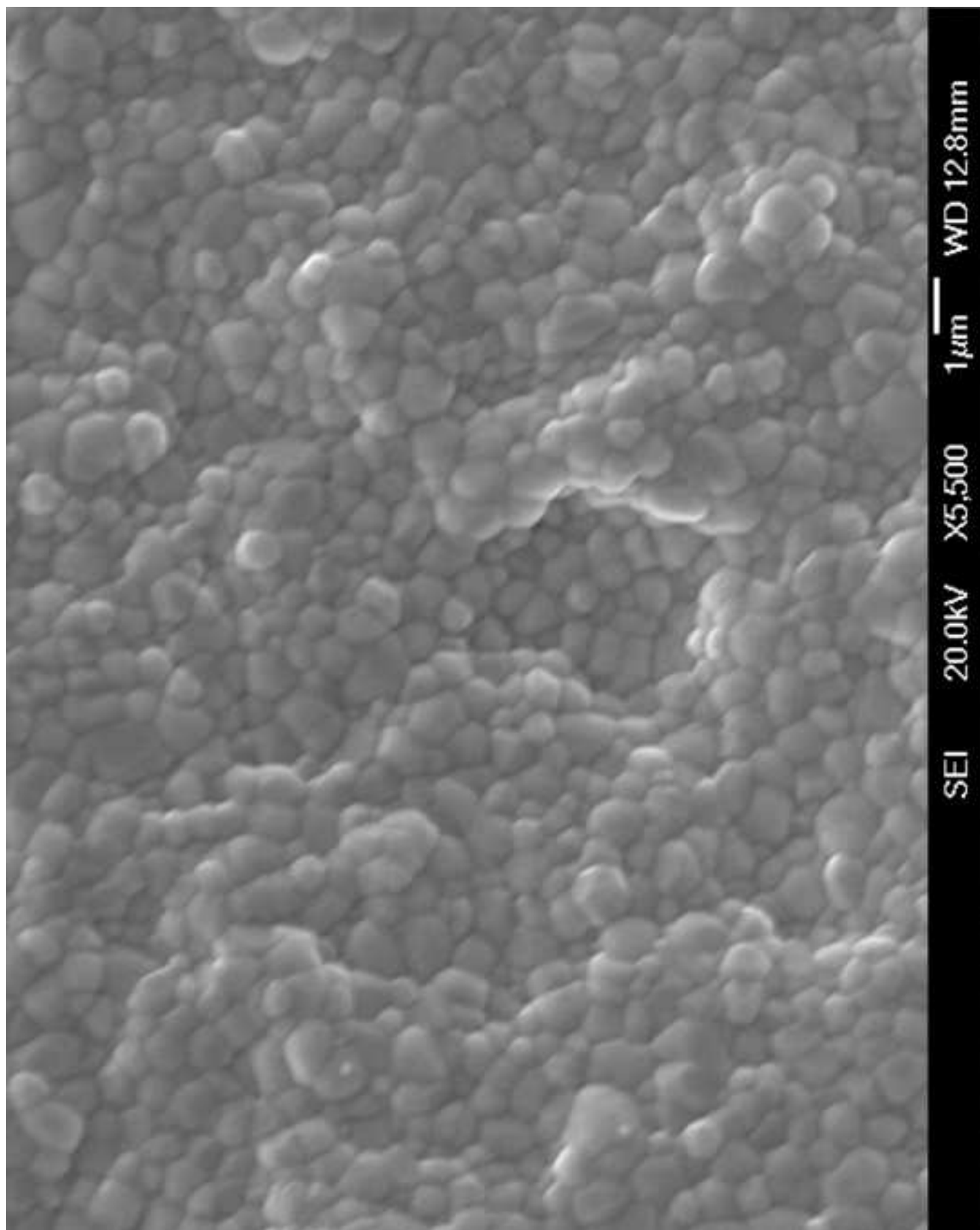


Figure 5(b)

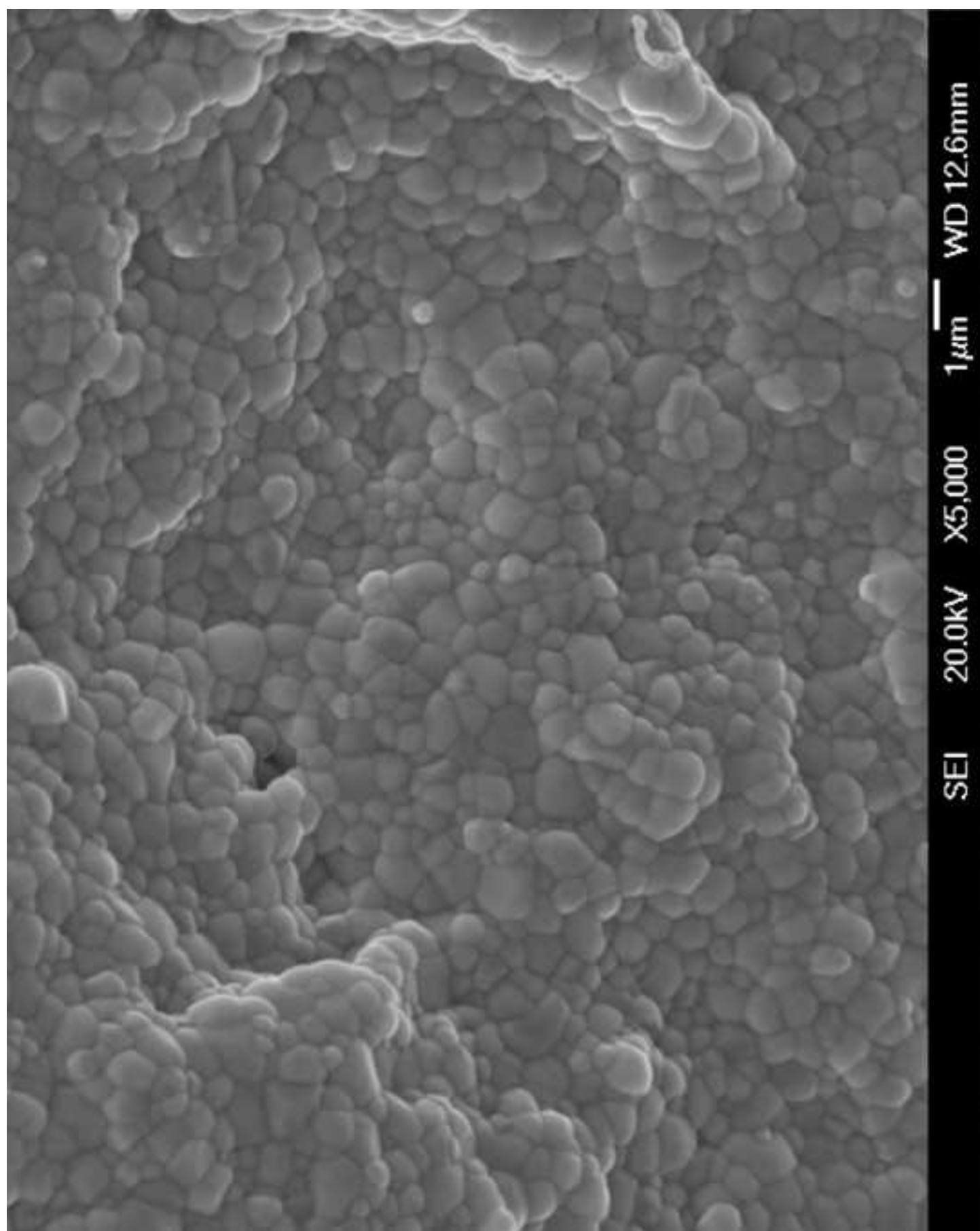


Figure 5(c)

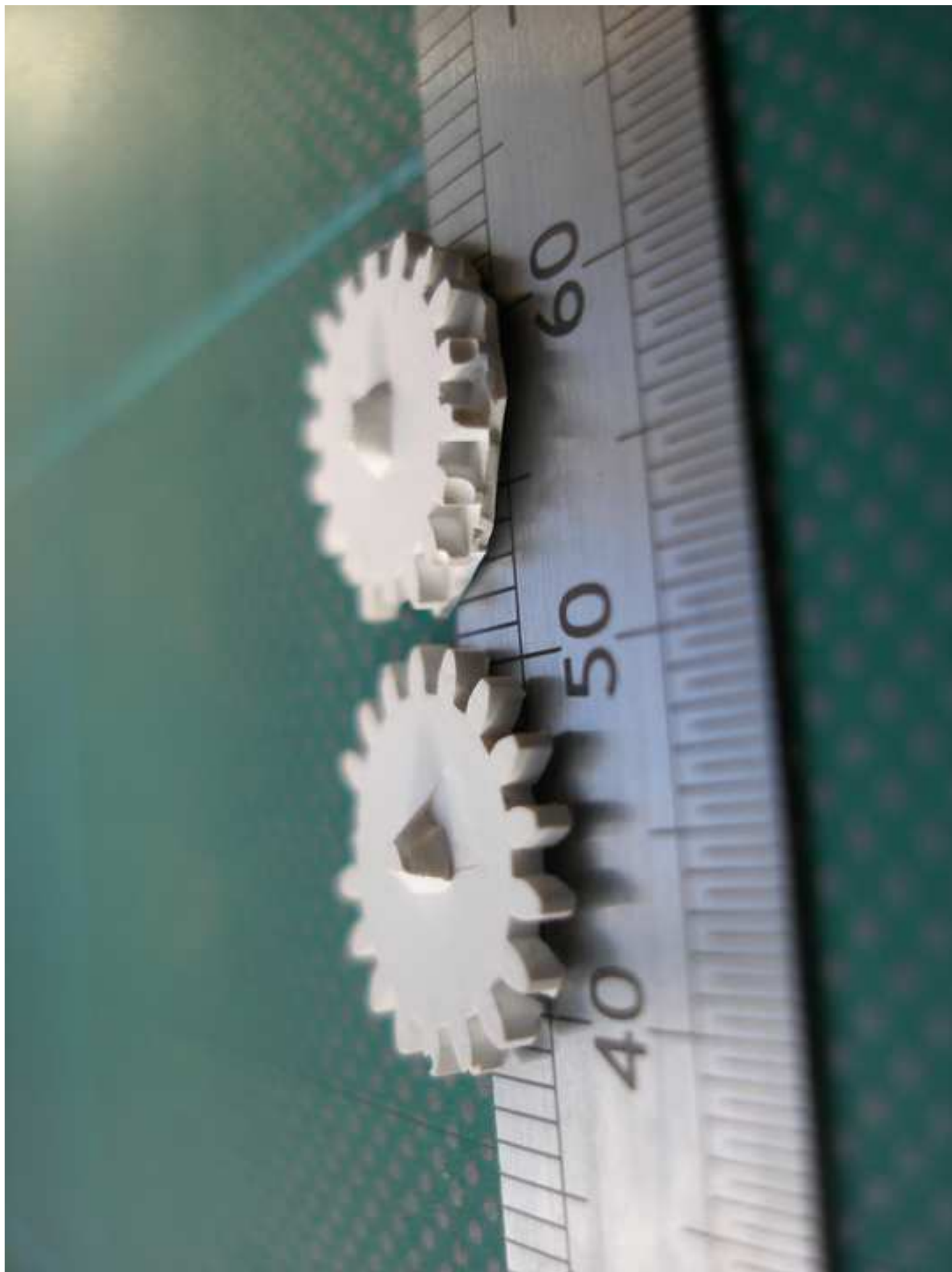


Figure 6

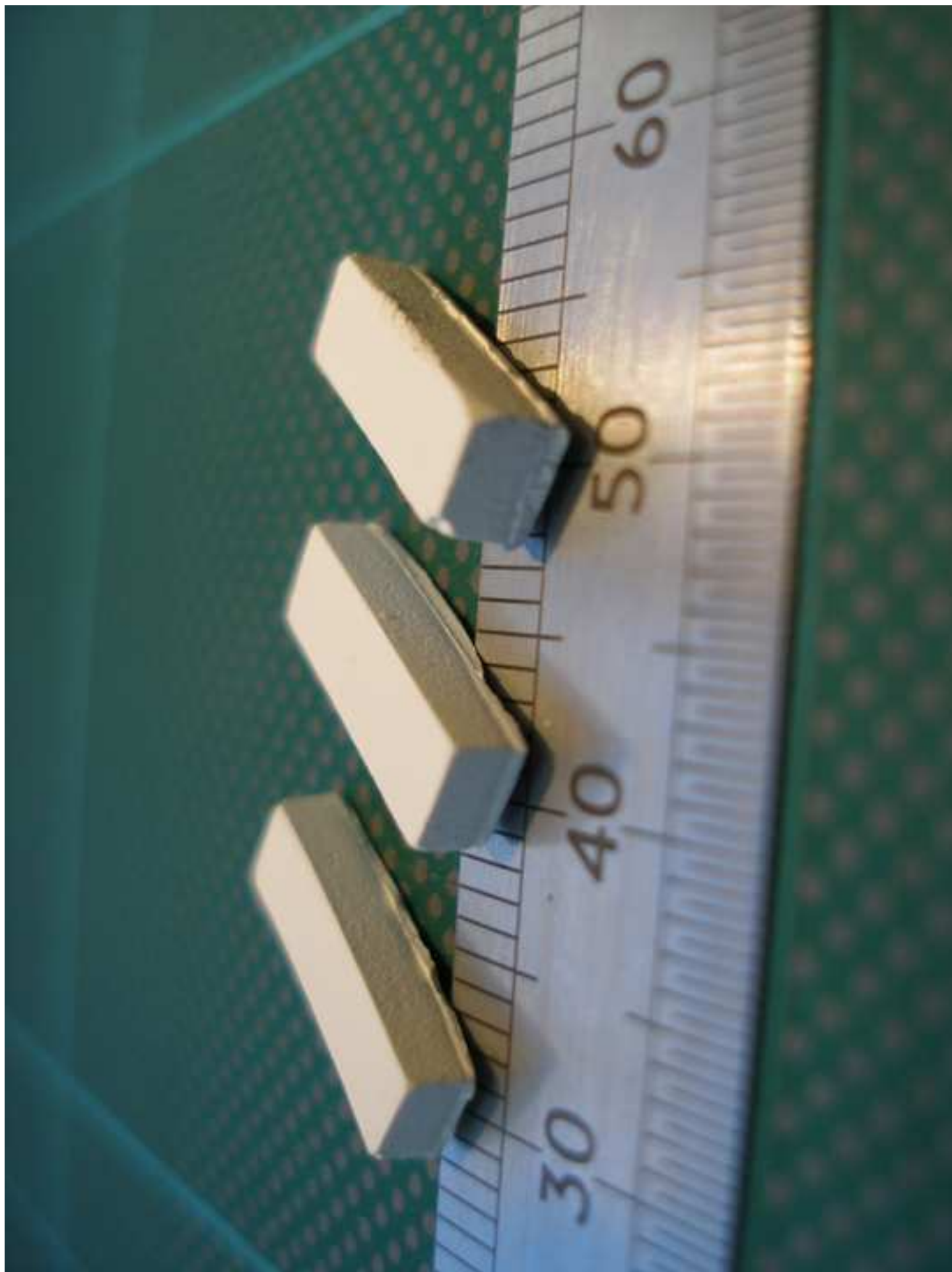


Figure 7

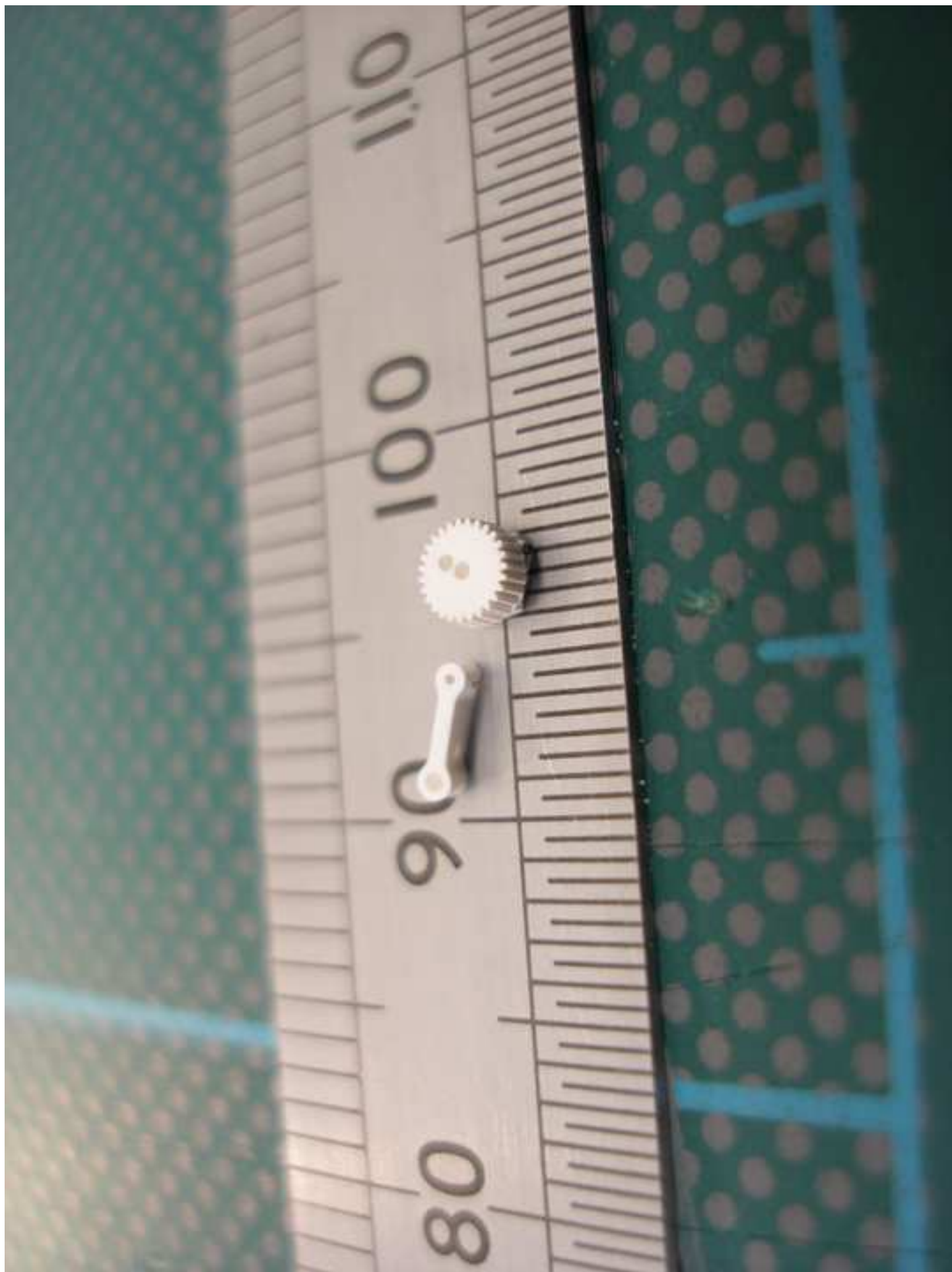


Figure 8